

X-ray diffraction study of amorphous $\text{Al}_{77.5}\text{Mn}_{22.5}$ and $\text{Al}_{56}\text{Si}_{30}\text{Mn}_{14}$ alloys

E. MATSUBARA, K. HARADA, Y. WASEDA

The Research Institute of Mineral Dressing and Metallurgy (SENKEN), Tohoku University, Sendai 980, Japan

H. S. CHEN

AT&T Bell Laboratories, Murray Hill, New Jersey 07974, USA

A. INOUE, T. MASUMOTO

The Research Institute for Iron, Steel, and Other Metals, Tohoku University, Sendai 980, Japan

The structure of amorphous sputtered $\text{Al}_{77.5}\text{Mn}_{22.5}$ and as-spun $\text{Al}_{56}\text{Si}_{30}\text{Mn}_{14}$ alloys is investigated by X-ray diffraction. Some distinct features are observed in the intensity profile, i.e. a pronounced prepeak at $Q = 16 \text{ nm}^{-1}$ in both the alloys and a shoulder at the low- Q side in Al-Si-Mn. Also in the radial distribution functions, the first peak has a shoulder at the high- r side. This experimental evidence suggests the presence of a strong chemical short-range order persisting in the α phase.

1. Introduction

Elser and Henley [1] and Guyot and Audier [2] have suggested that the structure of α -($\text{Al}_{73}\text{Si}_{10}\text{Mn}_{17}$) can be described in two different ways: a bcc-type packing of Mackay's icosahedral clusters [3], and a periodic packing of decorated three-dimensional Penrose rhombohedra. These two pictures of the α -phase have immediate relevance to models for the icosahedral phases. Measurements of extended X-ray absorption fine structure [4] showed a close resemblance between the α phase and icosahedral $\text{Al}_{74}\text{Si}_6\text{Mn}_{20}$. Observation of the as-spun $\text{Al}_{73}\text{Si}_{13}\text{Mn}_{14}$ alloy using a transmission electron microscope [5] revealed a definite orientation relationship between the α phase and the icosahedral Al-Si-Mn phase. These experiments indicate that the formation of icosahedral Al-Si-Mn by rapid solidification is correlated with the structural similarity of the equilibrium α phase. Furthermore, Koskenmaki *et al.* [5] suggested that icosahedral short-range order resembling that in the α phase and icosahedral phase exists in glassy alloys to explain the vitrification of as-spun $\text{Al}_{86-x}\text{Si}_x\text{Mn}_{14}$ over a large composition range. EXAFS measurements [6] showed the similarity of the local atomic structure around a manganese atom in icosahedral and amorphous Al-Mn alloys. Chen *et al.* [7] observed a prepeak and a shoulder on the main peak in the X-ray intensity profile of amorphous $\text{Al}_{66}\text{Si}_{20}\text{Mn}_{14}$. They concluded that these features could be associated with the local atomic configuration of α -(Al-Si-Mn), and that the icosahedral short-range order that exists in the α phase persists in the amorphous alloy. Consequently, quantitative measurements and analysis of the scattering intensity from these amorphous aluminium alloys should prove useful to reveal further details of the local atomic structure of these clusters.

In this paper, we report our X-ray diffraction study on amorphous sputtered $\text{Al}_{77.5}\text{Mn}_{22.5}$ and as-spun $\text{Al}_{56}\text{Si}_{30}\text{Mn}_{14}$ alloys.

2. Experimental procedure

Amorphous $\text{Al}_{77.5}\text{Mn}_{22.5}$ alloy was prepared by radio-frequency sputtering in the form of plates about 0.1 mm thick. For the X-ray measurements its surface was mechanically polished with an MgO-H₂O slurry. Amorphous $\text{Al}_{56}\text{Si}_{30}\text{Mn}_{14}$ alloy was obtained as a ribbon with about 1 mm wide and 17 μm thick by melt-spinning on a copper wheel in an argon atmosphere. Since this ternary sample was very brittle, short pieces of the ribbon were closely arranged between frames and put on top of one another, so that the sample used for the X-ray measurements was about 5 mm wide and ten layers thick. Details of the sample preparation are described elsewhere [5, 8].

A molybdenum X-ray rotating target operated at 50 kV and 180 mA, and a germanium 111 flat single-crystal monochromator in the incident beam were used. Intensity was detected by a scintillation counter with a pulse-height analyser. The intensity profile was obtained from 7 to 153 nm^{-1} in the wave-vector $Q = 4\pi \sin \theta/\lambda$, where 2θ is the angle between the incident and diffracted beams and λ is the wavelength. In order to extract only intensity from the sample from the total intensity, which includes intensity from the copper plate under the Al-Mn, X-rays were directed on to the sample surface at a very shallow angle of incidence, i.e. 2° in the present measurement, and only the detector was scanned. Intensity from the copper plate in identical experimental conditions was corrected for the absorption by the sample and subtracted from the total intensity. This resultant intensity was used for further analysis in Al-Mn. On the other hand, for

Al–Si–Mn a symmetrical transmission geometry was used. A fixed-count mode was applied and at least 20 000 counts were collected at every measured point in both the samples, so that the statistical counting error was $\pm 0.5\%$. The polarization correction for an ideally perfect monochromator was applied, and the Compton scattering was corrected using the values reported by Cromer and Mann [9] and the so-called Breit–Dirac recoil factors. In order to convert the observed intensities into electron units, the generalized Krogh–Moe–Norman method [10] was used with atomic scattering factors [11] including anomalous dispersion corrections [12]. In this work, the observed intensity data at Q values below 7 nm^{-1} were smoothly extrapolated to $Q = 0$. The effect of the extrapolation and the truncation up to $Q = 153 \text{ nm}^{-1}$ is known to give no critical contribution to the radial distribution function (RDF) calculated by Fourier transformation [13, 14]. The RDF is evaluated from the total structure factor $S(Q)$ for a non-crystalline system containing more than two kinds of atom by the equations

$$4\pi r^2 \rho(r) = 4\pi r^2 \rho_0 + \frac{2r}{\pi} \int_0^\infty Q [S(Q) - 1] \times \sin(Qr) dQ \quad (1)$$

$$S(Q) = [I_{\text{cu}}^{\text{coh}}(Q) - \langle f^2 \rangle + \langle f \rangle^2] / \langle f \rangle^2 \quad (2)$$

$$\langle f^2 \rangle = \sum_i c_i f_i^2 \quad (3)$$

$$\langle f \rangle = \sum_i c_i f_i \quad (4)$$

where $I_{\text{cu}}^{\text{coh}}(Q)$ is the coherent X-ray scattering intensity in electron units per atom, which is directly determined from the scattering experiments. f_i and c_i are the atomic scattering factor and the concentration, respectively, of the i th element. $\rho(r)$ is the averaged radial density function and ρ_0 is the average number density of atoms.

3. Results and discussion

Fig. 1 shows the X-ray scattering intensity patterns of amorphous Al–Mn and Al–Si–Mn, and the fundamental features of both profiles corresponds to a typical non-crystalline structure. Some distinct features are observed. For example, a pronounced prepeak appears at $Q = 16 \text{ nm}^{-1}$ in both alloys. In Al–Si–Mn, a marked shoulder at the low- Q side of the main peak is also visible. In general, the presence of a prepeak corresponds to compound-forming behaviour and the partial structure factor of unlike-atom pairs has a very sharp first peak with a prepeak [14–16]. The same features were observed in an amorphous $\text{Al}_{66}\text{Si}_{20}\text{Mn}_{14}$ alloy by Chen *et al.* [7]. They attributed these features to the presence of chemical short-range order. The structure factors $S(Q)$ of Al–Mn and Al–Si–Mn are given in Fig. 2. In addition to the features discussed above, quite clear splitting of the second peak as well as fairly distinct oscillations at high- Q region are rather unlike the patterns which are normally obtained in typical amorphous alloys. These also imply the presence of chemical short-range order in the alloys.

The RDFs calculated by Equation 1 are shown in Fig. 3. The notable features in these RDFs are the

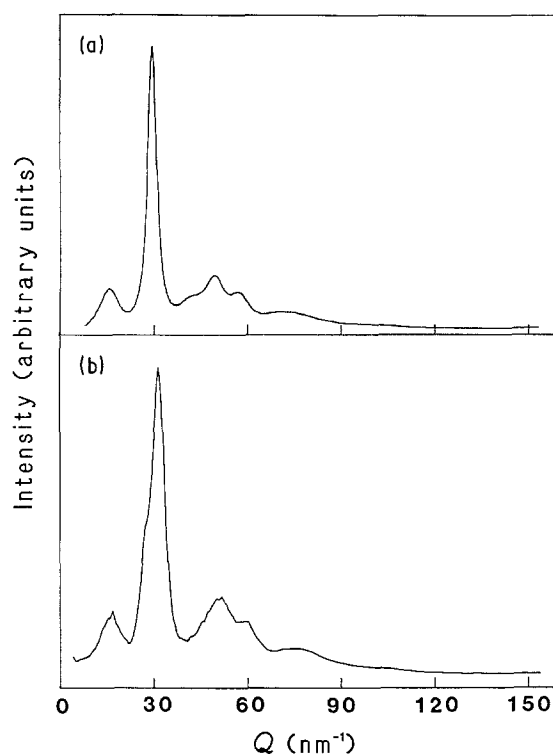


Figure 1 X-ray diffraction patterns for (a) amorphous sputtered $\text{Al}_{77.5}\text{Mn}_{22.5}$ and (b) as-spun $\text{Al}_{56}\text{Si}_{30}\text{Mn}_{14}$.

appearance of a marked shoulder at the high- r side of the first peak and the relatively strong undulation of the RDF curves over the large- r range, compared with the results from typical amorphous alloys. These RDFs give more obvious evidence of short-range ordering in these amorphous alloys. The spurious ripples in the small- r region are meaningless, since the RDF is essentially zero inside the atomic diameter. The right-skewed first peaks in both systems were

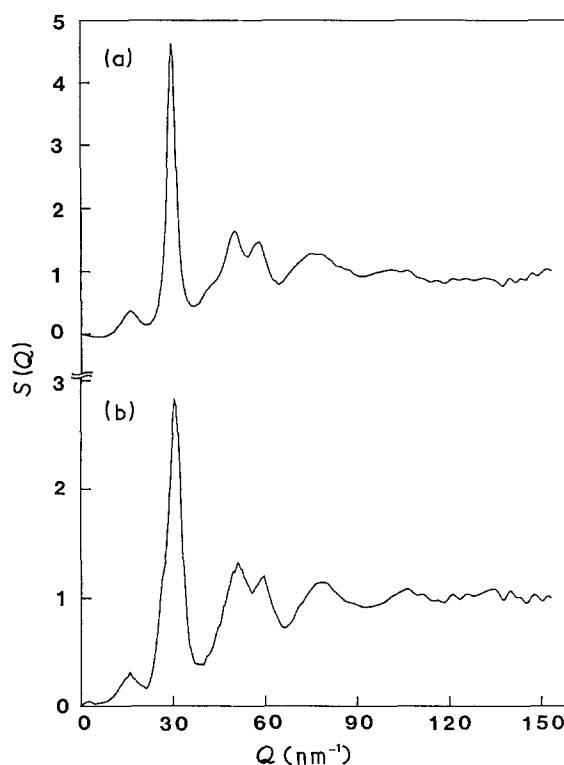


Figure 2 Total structure factors $S(Q)$ of (a) amorphous sputtered $\text{Al}_{77.5}\text{Mn}_{22.5}$ and (b) as-spun $\text{Al}_{56}\text{Si}_{30}\text{Mn}_{14}$.

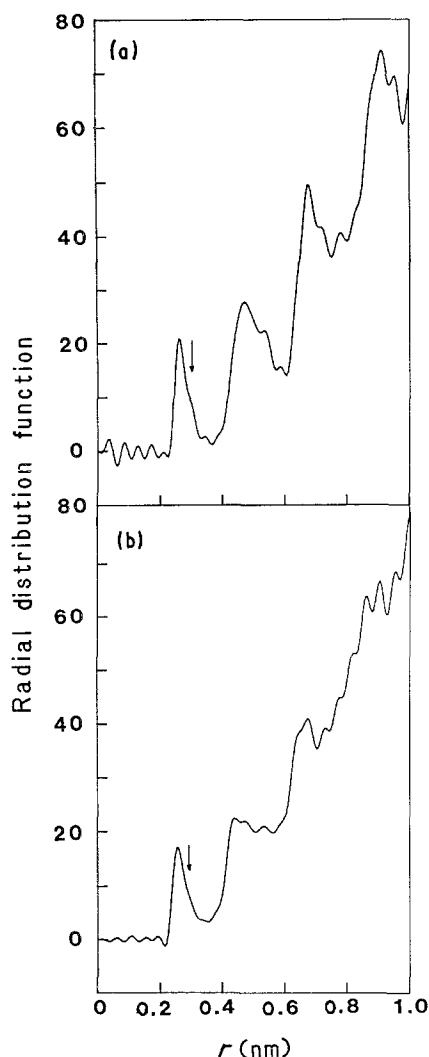


Figure 3 Radial distribution functions of (a) amorphous $\text{Al}_{77.5}\text{Mn}_{22.5}$ (density = 3.50 g cm^{-3}) and (b) as-spun $\text{Al}_{56}\text{Si}_{30}\text{Mn}_{14}$ (density = 3.25 g cm^{-3}). The arrows indicate the shoulder at the first peak.

fitted by assuming that the shapes of the peaks around their maximum and shoulder are Gaussian. The peak positions were determined from the positions of the apexes of the fitted curves, and the coordination numbers were evaluated from the areas under the curves. An error for the coordination number is about $\pm 8\%$ at most. The results are summarized in Table I, together with the values calculated from the structural data for α - $(\text{Al}_{77.5}\text{Si}_{10.1}\text{Mn}_{17.4})$ [17]. These for the α phase were the average over all possible Mn–Al(Si) (or Al(Si)–Mn) and Al(Si)–Al(Si) pairs in the unit cell. Since the X-ray scattering factors for these elements are nearly equal, we can not distinguish between aluminium and silicon. Thus, all atoms around manganese will be called aluminium.

In Table I, taking account of experimental error, we can see that the positions of the two peaks experimen-

tally determined show a fairly good agreement with those for the Mn–Al and Al–Al pairs of the α phase. For the Mn–Al pairs, the coordination numbers also accord with that of the α phase. As discussed in the introduction, Chen *et al.* [7] and Boyce *et al.* [6] implied the presence of icosahedral short-range clusters in amorphous Al–Si–Mn and Al–Mn, respectively. Thus, in order to explain the present results, it seems that icosahedral clusters similar to those constructing the α phase are appropriate as short-range order in the present case. The α - (Al–Si–Mn) phase is almost body-centred, belonging to the space group $\text{Pm}\bar{3}$ [17]. There are two types of manganese atom, Mn_1 and Mn_2 [18]. The manganese atoms belonging to each group are positioned at the vertices of an icosahedron surrounding the vacant site at the origin and centre of the unit cell, respectively. The interatomic distance between manganese atoms calculated from the crystal structural data of the α phase is 0.505 nm on the average. Aluminium atoms also form an icosahedron inside the manganese icosahedron. The average distances between aluminium and manganese, as well as aluminium and aluminium, are already tabulated in Table I.

The distinct feature of the diffraction profile observed in both the alloys was the prepeak. To explain its cause by the icosahedral short-range clusters proposed must be a good criterion to prove the validity of the present model. An empirical relation between the correlation length, r , in real space and the peak position, Q , in the intensity profile, $Qr = 2.5\pi$, is known in molten transition metals and metalloid alloys [14]. Based on the fact that the general structural features of the amorphous state are similar to those of the liquid state, it is plausible that the above relation is still valid even in the amorphous state. Thus, a correlation length causing the prepeak at 16 nm^{-1} was estimated to be 0.491 nm , which shows a remarkable agreement with the Mn–Mn distance calculated from the icosahedron in the α phase.

From this X-ray diffraction study in amorphous Al–Mn and Al–Si–Mn, a distinct prepeak at about $Q = 16 \text{ nm}^{-1}$ was confirmed. In Al–Si–Mn, a shoulder on the low- Q side of the main peak at $Q = 27 \text{ nm}^{-1}$ is also observed. The existence of the prepeak suggests a strong chemical short-range order and is ascribed to Mn–Mn pairs positioned at the vertices of the icosahedral clusters at an average distance of 0.491 nm . The first peak of the RDF has a shoulder on the large- r side of the main peak. The main peak and shoulder are attributed to an Mn–Al pair and an Al–Al pair, respectively, on the assumption that the icosahedral short-range clusters are similar to those in the α phase. Consequently, the present results strongly suggest that the atomic structure of amorphous $\text{Al}_{77.5}\text{Mn}_{22.5}$ and

TABLE I Comparison of coordination numbers, N , and interatomic distances, r , for amorphous $\text{Al}_{77.5}\text{Mn}_{22.5}$ and $\text{Al}_{56}\text{Si}_{30}\text{Mn}_{14}$ obtained in this study with those calculated from the α phase [17].

Alloy	Mn–Al(Si)		Al(Si)–Mn		Al(Si)–Al(Si)	
	r (nm)	N	r (nm)	N	r (nm)	N
Amorphous sputtered $\text{Al}_{77.5}\text{Mn}_{22.5}$	0.260	10.9	0.260	3.16	0.295	7.77
Amorphous as-spun $\text{Al}_{56}\text{Si}_{30}\text{Mn}_{14}$	0.254	10.9	0.254	1.77	0.284	7.95
α - $(\text{Al}_{77.5}\text{Si}_{10.1}\text{Mn}_{17.4})$	0.267	11.5	0.267	2.42	0.283	10.1

Al₅₆Si₃₀Mn₁₇ alloys could be described as a dense random packing of the Mackay icosahedra proposed by Chen *et al.* [7].

References

1. V. ELSER and C. L. HENLEY, *Phys. Rev. Lett.* **55** (1985) 2883.
2. P. GUYOT and M. AUDIER, *Phil. Mag.* **B52** (1985) L15.
3. A. L. MACKAY, *Acta Crystallogr.* **15** (1962) 916.
4. M. A. MARCUS, H. S. CHEN, G. P. ESPINOZA and C. L. TSAI, *Solid State Commun.* **58** (1986) 1659.
5. D. C. KOSKENMAKI, H. S. CHEN and K. V. RAO, *Phys. Rev. B* **33** (1986) 5328.
6. J. B. BOYCE, F. G. BRIDGES and J. J. HAUSER, *J. Physique* **47** (1986) C8-1029.
7. H. S. CHEN, D. KOSKENMAKI and C. H. CHEN, *Phys. Rev. B* **35** (1987) 3715.
8. A. INOUE, K. MATSUZAKI, T. OGASHIWA and T. MASUMOTO, *J. Mater. Sci.* **22** (1987) 2063.
9. D. T. CROMER and J. B. MANN, *J. Chem. Phys.* **47** (1967) 1892.
10. C. N. J. WAGNER, H. OCKEN and M. L. JOSHI, *Z. Naturforsch.* **20a** (1965) 325.
11. International Tables for X-ray Crystallography, Vol. IV (Kynoch, Birmingham, 1974) p. 99.
12. D. T. CROMER and D. LIBERMANN, *J. Chem. Phys.* **53** (1970) 1891.
13. C. N. J. WAGNER, *J. Non-Cryst. Solids* **31** (1978) 1.
14. Y. WASEDA, "The Structure of Non-Crystalline Materials" (McGraw-Hill, New York, 1980) p. 60.
15. H. F. BUHNER and S. STEEB, *Z. Naturforsch.* **24a** (1969) 428.
16. S. STEEB and R. HEZEL, *Z. Metallkde* **57** (1963) 374.
17. M. COPPER and K. ROBINSON, *Acta Crystallogr.* **20** (1966) 614.
18. W. B. PEARSON, "Handbook of Lattice Spacings and Structure of Metals" (Pergamon, New York, 1967) p. 375.

*Received 29 May
and accepted 27 July 1987*